Green Chemical Technology

SCIEPublish

Article

Green Synthesis of $NiFe_2O_4$ Nanoparticles Using Combretum Indicum Leaf Extract for the Synthesis of 2-Aryl Benzimidazole

Kalpana Tekale [1] and Santosh Katkar [2,*]

[1] M.S.P. Mandal's Shivchhatrapati College, Chhatrapati Sambhajinagar 431003, Maharashtra, India; kalpanatekale1@gmail.com (K.T.)

[2] Chemistry Research Centre, MSS'S Arts, Science and Commerce College, Ambad, Jalna 431204, Maharashtra, India

* Corresponding author. E-mail: katkars25@gmail.com (S.K.)

Received: 23 May 2026; Revised: 10 June 2026; Accepted: 14 July 2026; Available online: 3 August 2026

ABSTRACT: The versatile applications of nitrogen-containing heterocycles in different industries have engendered a lot of research. Benzimidazole derivatives, as isostructural pharmacophores of naturally occurring active biomolecules, are popular chemotherapeutic drugs. The present study focuses on a green methodology for the synthesis of $NiFe_2O_4$ nanocomposite using Combretum indicum leaf extract, and for the synthesis of 2-aryl benzimidazole derivatives via the condensation of aromatic aldehydes and *O*-phenylenediamine. The synthesized catalyst was characterized through various analytical techniques, including FT-IR, XRD, SEM, TEM, and BET. It has several advantages, including a rapid reaction at room temperature, easy work-up, high product yield, simple purification, and a reusable catalyst. The catalyst was reused for up to six consecutive cycles, with the yield decreasing only marginally from 95% (fresh catalyst) to 89% (sixth reuse).

Keywords: Benzimidazoles; $NiFe_2O_4$; Combretum indicum extract; Green method

1. Introduction

The key advantage of magnetic nanoparticles is that they can be easily removed from the reaction by using an external magnet. Also, this magnet assisted catalyst recovery saves catalyst loss, time, and energy [1]. These days, a lot of research is going on to produce nanoscale metals by physical, chemical, and environmentally friendly methods [2,3].

Green synthesis is gradually replacing physical and chemical methods due to the excessive energy consumption [3,4], the release of toxic and harmful chemicals [5], and the complexity of the equipment and synthesis conditions [6,7], Extracts from leaves are currently the most common green source for synthesis [8–10], flower roots [11–13], peelings [14], fruits [15] and seeds of different plants [16,17]. However, the wide range of phytochemicals in plant extracts can effectively reduce a great number of metal ions and also aid in the green synthesis of nanoparticles [18].

Plant extracts are a key component in the preparation of nanoparticles due to their benefits and special properties, and are a more economical, efficient, and environmentally friendly way of producing nanoparticles than by chemical and physical methods [19,20]. Several phytochemicals, including terpenoids, flavonoids, ketones, aldehydes, amides, and carboxylic acids, are present in the leaves and act as stabilizers and reducing agents during the synthesis of metal and metal oxide nanoparticles [19]. In particular, plant extracts are often employed in nanoparticle synthesis due to their affordability, environmental friendliness, and ability to produce biocompatible, enhanced nanoparticles. Plant extracts play a key role in the preparation of nanoparticles [21–23]. So, plant extract-induced synthesis of $NiFe_2O_4$ nanoparticles was considered in this study. Plant extracts contain phytochemicals that act as natural reducing agents and stabilizers to form toxic free biocompatible nanoparticles.

Due to their variety of pharmacological actions and medicinal chemistry applications, 2-aryl benzimidazole synthesis is important [24,25]. These substances have been widely studied due to their various biological activities, including antibacterial, antifungal, antiviral, anticancer, and antihistamine properties [26]. Several benzimidazole compounds have been synthesized with antimicrobial [27], anticancer [28], anti-inflammatory [29], analgesic [30], antimalarial [31], antitubercular [32], antiviral [33], antihistaminic [34], anti-HIV [35], acetylcholinesterase [36], and antiprotozoal [37] activities. Further investigation into 2-aryl benzimidazoles might result in the development of more potent and therapeutically useful substances for the treatment of a range of diseases [38]. The popularity of these molecules in drug discovery is enhanced by the development of eco-friendly and efficient synthesis methods using ionic liquids, $AlCl_3$, or magnetic nanocatalysts [39–41].

While plant-extract-mediated green synthesis of magnetic ferrite nanoparticles is well established, reports specifically employing Combretum indicum leaf extract to fabricate $NiFe_2O_4$ remain scarce, underscoring the novelty of the approach described here. Bio-inspired synthesis of related binary and multicomponent oxide nanomaterials, including zinc ferrite, zinc tin oxide, nickel ferrite, bismuth ferrite, and zinc zirconate, has likewise been demonstrated using natural plant extracts as green chelating agents [42–46], further supporting the broader applicability of phyto-mediated routes to magnetically active spinel oxides such as the $NiFe_2O_4$ nanocatalyst reported in the present work.

2. Results and Discussion

The catalyst loading had a marked impact on the model reaction of 4-hydroxybenzaldehyde and o-phenylenediamine. Increasing the $NiFe_2O_4$ from 5 to 20 mg also increased the yield (62–95%) and reduced the reaction time (90–40 min) since more active sites were available. The best catalytic activity was found to be 20 mg $NiFe_2O_4$ (Table 1 entry 4). No further improvement was made with 25 mg of catalyst, so 20 mg is the best catalyst loading.

Table 1. Effect of catalyst loading.

Entry	Catalyst Amount (mg)	Reaction Time (min) [a]	Yield (%) [b]
1	5	90	62
2	10	70	78
3	15	50	90
4	20	40	95
5	25	40	95

[a] Reaction conditions: 4-hydroxybenzaldehyde (1 mmol), o-phenylenediamine (1 mmol), catalyst (20 mg), and ethanol 10 mL; [b] Isolated yields.

Table 2 shows that aldehydes containing both electron-donating and electron-withdrawing groups produced the desired products with good to excellent yields (87–95%) within 30–45 min, indicating broad substrate scope and efficiency of the reaction. The observed melting points closely matched the reported values, confirming both the purity and identity of the synthesized compounds.

Table 2. Synthesis of 2-phenyl-1H-benzimidazole derivatives using $NiFe_2O_4$ NPs catalyst.

Sr. No.	Aldehyde	Product	Yield (%)	Time (Min)	M. P. (°C)	
					Observed	Reported
3a	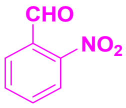	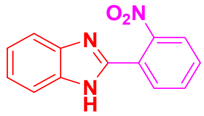	92	35	117–119	118–120 [40]
3b	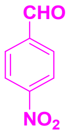	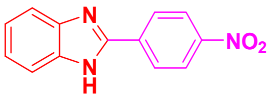	93	30	309–311	312–314 [40]
3c	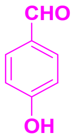	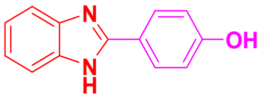	95	40	195–197	196–198 [41]
3d	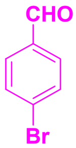	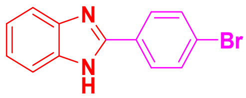	89	50	245–247	250–252 [40]
3e	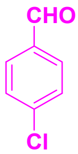	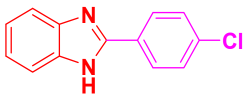	87	45	285–286	289–290 [40]

Next, we have compared the catalyst with other reported catalysts (Table 3). The $NiFe_2O_4$ catalyst is more efficient than the reported catalysts, with yields of 87–95% in 35–50 min under mild conditions. In contrast, other catalysts require much longer reaction times and much harsher reaction conditions.

Table 3. Comparison of the catalyst with other reported catalysts.

Entry	Catalyst	Condition	Reaction Time (min)	Yield (%)	References
1	Silica-supported periodic acid	RT with acetonitrile	12–35 min	70–95	[47]
2	NH_4Cl	80 °C in ethanol	2.5–4 h	68–84	[48]
3	MgO@DFNS	RT in ethanol	180 min	82–94	[49]
4	$NiFe_2O_4$	RT in ethanol	35–50 min	87–95	Present work

Protic solvents play a beneficial effect in encouraging condensation and cyclization; ethanol produced the highest yield (95%) in the shortest time (40 min), followed by methanol (88%, 50 min) and water (82%, 52 min). Less successful were acetonitrile (75%, 60 min) and toluene (80%, 55 min). As a result, ethanol was chosen as the best solvent, taking into account green chemistry, yield, and efficiency (Table 4).

Table 4. Effect of solvent on the synthesis of 2-(4-hydroxyphenyl) benzimidazole.

Entry	Solvent	Reaction time (min)	Yield (%)
1	Ethanol	40	95
2	Methanol	50	88
3	Water	52	82
5	Acetonitrile	60	75
6	Toluene	55	80

The recyclability of the $NiFe_2O_4$ catalyst was investigated by the same model reaction. It was easily recovered by filtration and washed for reuse (Table 5 and Figure 1). The catalyst remained active in six cycles without deactivation. Consistent high yields were obtained, similar to those with a new catalyst.

Table 5. Reusability study of the catalyst.

Cycle Number	Yield (%)
Fresh	95
1st reuse	94
2nd reuse	93
3rd reuse	92
4th reuse	91
5th reuse	90
6th reuse	89

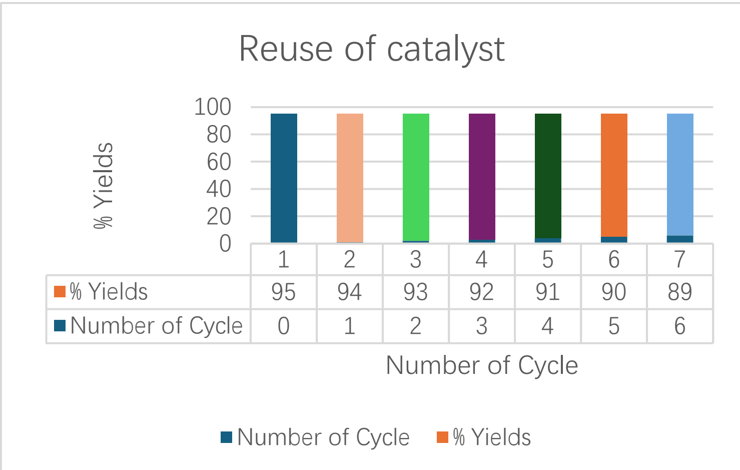

Figure 1. Recovery and reusability of $NiFe_2O_4$ nanocatalyst.

3. Experimental

3.1. Materials and Methods

Nickel(II) nitrate hexahydrate ($Ni(NO_3)_2{\cdot}6H_2O$, ≥99%) and iron(III) nitrate nonahydrate ($Fe(NO_3)_3{\cdot}9H_2O$ as precursor salts. The reagents were obtained from Sigma-Aldrich (St. Louis, MO, USA)) and used without further purification. The reaction progress was monitored by Thin Layer Chromatography (TLC). Melting points of the products were measured by a digital melting point apparatus. The synthesized products were characterized by ^1H NMR (500 MHz, $CDCl_3$/DMSO, TMS) on a Bruker Avance Neo 500 spectrometer at the Sophisticated Analytical Instrumentation Facility (SAIF), Chandigarh University, Mohali, India. The mass spectra were obtained on a Shimadzu-GCMS-QP2010 spectrometer operating at 70 eV.3.2. Preparation of Plant Extract.

3.2. Preparation of Plant Extract

The leaves of Combretum indicum were sourced from a local garden and washed with deionized water. About 10 g of leaves were cut into pieces and placed in 100 mL of deionized water, then heated at 70 °C. After cooling, the mixture was filtered, and the leaf extract was used for the synthesis of the nanoparticles.

Combretum indicum leaf extract appears to have a diverse phytochemical profile. Primary constituents of the extract include phenolic compounds and flavonoids such as gallic acid and rutin, along with alkaloids, saponins, tannins, and flavonoids like vitexin and orientin [50]. Metal ion coordination can also be achieved with the hydroxyl, aromatic, and carbonyl groups that are present in these phytochemicals. This suggests that the earliest stage of nanoparticle formation may involve the chelation of metal ions with the phenolics and flavonoids of the leaves via ion coordination, similar to previous reports of chelation-induced formation of metal oxide nanoparticles [51]. During the sol-gel auto-combustion of the metal–phytochemical complex, it is likely that the complex will undergo thermal decomposition, allowing the ligands to be expelled as gases and crystallizing the spinel $NiFe_2O_4$ structure. FT-IR spectra show a broad absorption near 3240 cm^{-1} along with weak bands near 1182 and 979 cm^{-1} (Section 4.4), which suggest that phytochemicals are present on the surface of the nanoparticles, where they may have a functional role.

3.3. Preparation of Nickel Ferrite Nanoparticles

Nickel ferrite nanoparticles were synthesized by sol–gel auto combustion using nickel nitrate hexahydrate [$Ni(NO_3)_2 \cdot 6H_2O$] and ferric nitrate. The metal nitrates were dissolved in 50 mL of deionized water, and 1 drop of Combretum indicum leaf extract was added dropwise while stirring at 80 °C, then heated until a gel. The dried gel was then annealed at 600 °C for 4 h to produce the final nickel ferrite nanoparticles.

3.4. Characterization of Nickel Ferrite Nanoparticles

Catalyst was analyzed by various methods through XRD, FT-IR, SEM, TEM, and BET analysis to check their structure, shape, and surface features. XRD confirmed phase purity and crystallite size, FT-IR spotted the key functional groups and the metal–oxygen bonds, while SEM and TEM showed their overall shape and nanoscale details. BET gave information about surface area and porosity, hinting that these particles could work well as catalysts.

3.5. Synthesis of 2-Aryl Benzimidazole Derivatives

A mixture of o-phenylenediamine (1 mmol) and the chosen aryl aldehyde (1 mmol) in a 25 mL round-bottom flask. Then, 20 mg of $NiFe_2O_4$ magnetic nanoparticles and 10 mL of ethanol as the solvent (Scheme 1). Then the mixture was stirred on a magnetic stirrer at room temperature, with progress monitored by TLC at regular intervals. Once the reaction finished, separated the catalyst with a magnet, washed it with ethanol, and dried it. After recrystallizing from ethanol gave good to excellent yields (Table 3, Entries 3a–e).

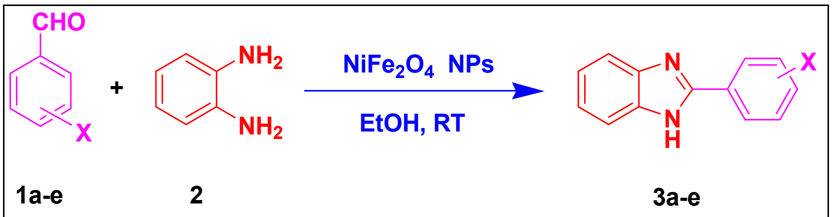

Scheme 1. Synthesis of 2-aryl benzimidazoles using $NiFe_2O_4$ NPs catalyst.

3.6. Spectral Data of the Representative Compounds

2-(2-Nitrophenyl)-1H-benzimidazole (3a): mp 117–119 °C; yield 92%; **FT-IR** (KBr, ν, cm^{-1}): 3739, 3040, 2526, 1797, 1604, 1519, 1341, 1421, 1267, 1223, 1066, 979, 916, 853, 764, 734. **^{1}H NMR** (500 MHz, DMSO-d_6, δ ppm):13.05 (s, 1H, N–H), 9.04–7.94 (m, 4H, Ar–H), 7.56–7.35 (m, 4H, Ar–H), 1.06 (s, 2H).

2-(4-Nitrophenyl)-1H-benzimidazole (3b): mp 309–311 °C; yield 93%; **FT-IR** (KBr, ν, cm^{-1}): 3711, 3649, 3297, 3014, 2906, 2680, 2320, 1653, 1595, 1506, 1432, 1328, 1096, 1009, 955, 844, 740, 693. **^{1}H NMR** (500 MHz, DMSO-d_6, δ ppm):13.29 (s, 1H, N–H), 8.83–8.44 (m, 4H, Ar–H), 8.40–7.60 (m, 4H, Ar–H).

2-(4-Hydroxyphenyl)-1H-benzimidazole (3c): mp 195–197 °C; yield 95%; **FT-IR** (KBr, ν, cm^{-1}): 3921, 2880, 2596, 1887, 1594, 1443, 1381, 1243, 1159, 1107, 893, 824, 736. **^{1}H NMR** (500 MHz, DMSO-d_6, δ ppm): 10.55 (s, 1H, N–H), 9.80 (s, 1H, O–H), 8.10–7.60 (m, 4H, Ar–H), 7.25–6.40 (m, 4H, Ar–H).

4. Characterization

4.1. XRD Analysis

From the XRD pattern of synthesized $NiFe_2O_4$ nanoparticles, the diffracted peaks are obtained at 2θ ≈ 30.2°, 35.5°, 43.2°, 53.6°, 57.2°, and 62.8°, corresponding to the (220), (311), (400), (422), (511), and (440) planes of the cubic spinel structure (JCPDS 10-0325). The absence of impurity peaks in the XRD pattern indicates the phase purity of the synthesized material (Figure 2).

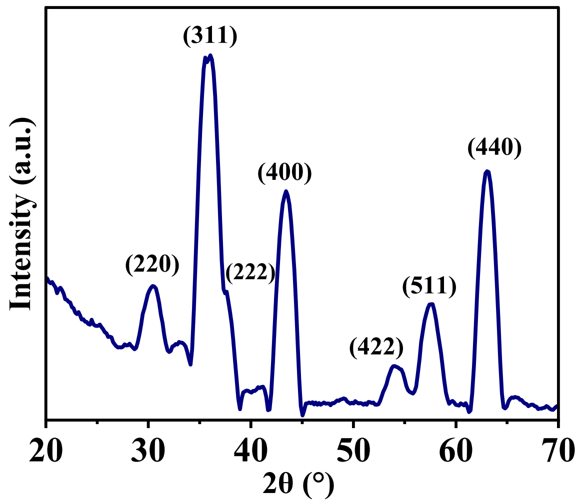

Figure 2. XRD analysis of $NiFe_2O_4$ nanoparticles.

4.2. SEM Analysis

SEM micrographs show particle distribution and surface morphology of $NiFe_2O_4$ nanoparticles at different magnifications. The images reveal that $NiFe_2O_4$ nanoparticles generally exhibited non-uniform, aggregated-nanostructured appearance with particle size distribution, and it resembles to most of the spinel ferrites (Figure 3).

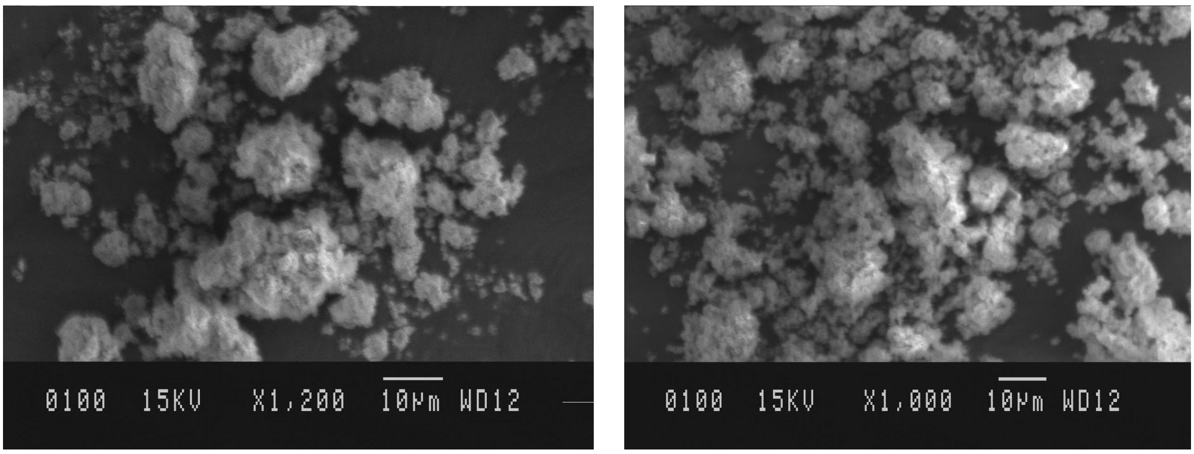

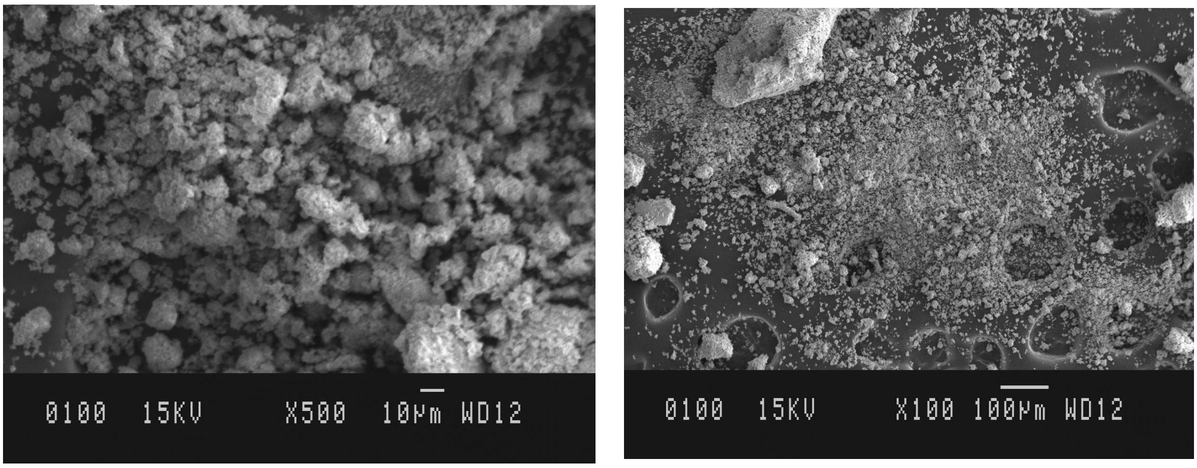

Figure 3. SEM images of $NiFe_2O_4$ nanoparticles.

4.3. HR-TEM

HR-TEM images of synthesized nickel ferrite nanoparticles shown quasi-spherical particles with a little aggregation owing to magnetic interaction. The nanoparticles show a uniform distribution with an average size of 12–18 nm. High resolution lattice fringe images show the clear appearance of planes. The obtained values correspond to the characteristic d-values of the $NiFe_2O_4$ spinel structure. The formation of the sharp and continues lattice fringes showed good crystallinity of the obtained nanoparticles (Figure 4).

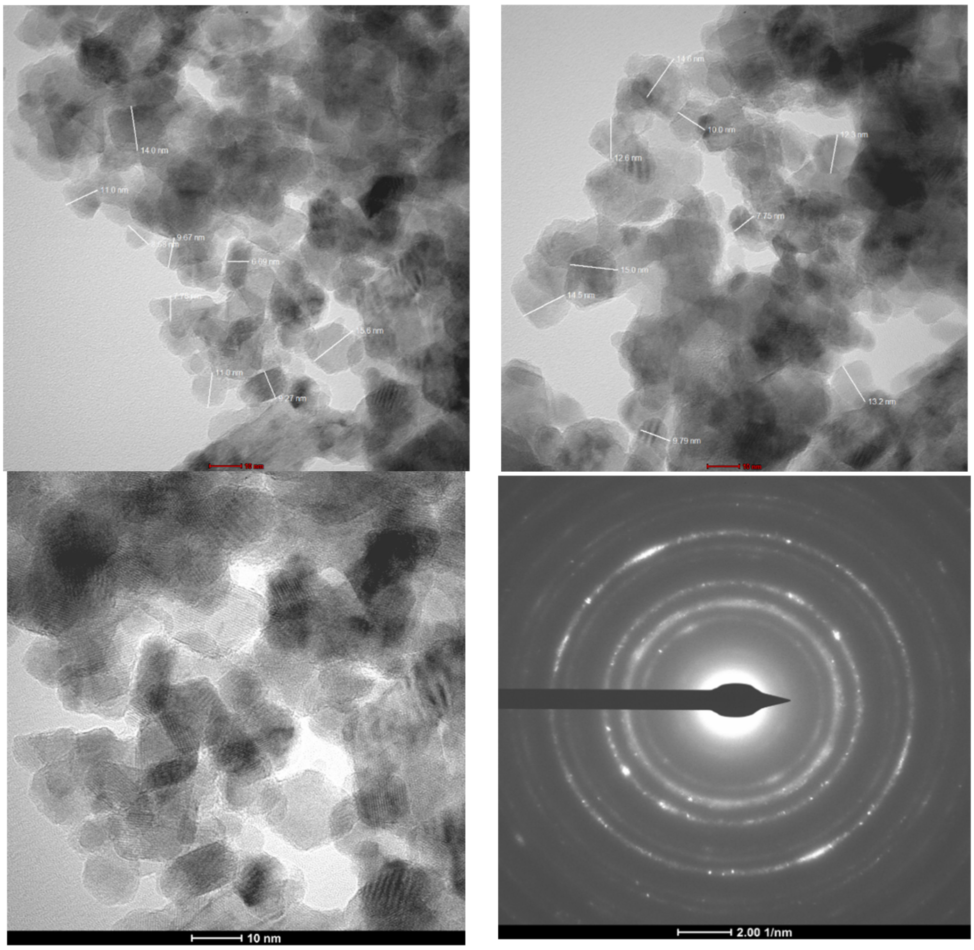

Figure 4. TEM images of $NiFe_2O_4$ nanoparticles.

4.4. FT-IR Analysis

The FT-IR spectra show a broad band at about ~3240 cm^{-1} due to adsorptive water/surface hydroxyls, and a band near ~1502 cm^{-1} may attributed to H–O–H bend or residual organic from the process. There were found very weak peaks at about ~1182 and ~979 cm^{-1}, attributed to surface organic group or adsorbed anions (Figure 5). Metal-oxygen characteristic vibration of spinel ferrite is located between the wave-number 400–600 cm^{-1} (Fe–O/Ni–O) located at the octahedral and tetrahedral sites, which confirms the formation of $NiFe_2O_4$. Adsorption water, surface hydroxyl groups, and surface organics on the surface show that there may exist incomplete surface coverages, which would affect its magnetic property and catalytic performance.

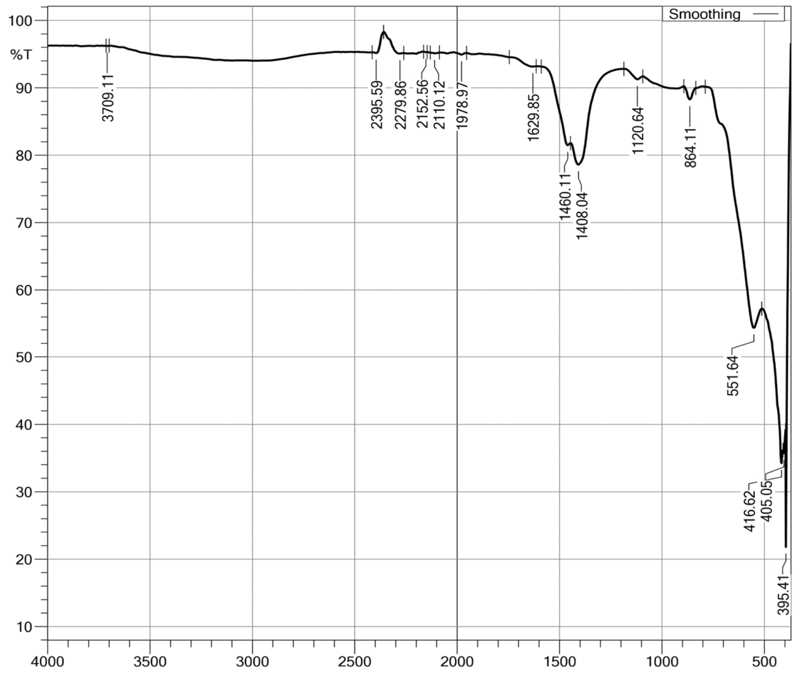

Figure 5. FTIR spectrum of $NiFe_2O_4$ nanoparticles.

4.5. BET Surface Area

NF1 had the nitrogen adsorption–desorption isotherm with a typical mesoporous type (Figure 6). BET analysis over a limited P/P_0 range (0.05–0.30) linear portion yielded a surface area of 49.82 m^2g^{-1} with a high correlation coefficient (r = 0.999987), confirming an excellent fit to the BET. There was no microporosity on the t-plot, which confirmed the material was mainly mesoporous. BJH desorption analysis showed a pore diameter of 6.17 nm and pore volume of 0.254 $cc\cdot g^{-1}$, with the total pore volume found at P/P_0 = 0.99356 was 0.251 $cc\cdot g^{-1}$. These results demonstrate that NF1 has a moderate surface area and well-defined mesoporosity, making it suitable for catalytic applications. Although 49.82 m^2g^{-1} is modest relative to high-surface-area supports such as mesoporous silica or carbon, it is comparable to, and slightly higher than, values reported for other plant-extract-mediated $NiFe_2O_4$ nanoparticles, such as the 46.73 m^2g^{-1} obtained for $NiFe_2O_4$ synthesized using Hydrangea paniculata flower extract [52]. This shows that the catalytic effectiveness found here is due to the high density and accessibility of active surface sites rather than an extremely large surface area, which is consistent with the mesoporous structure revealed by the BJH and t-plot analyse.

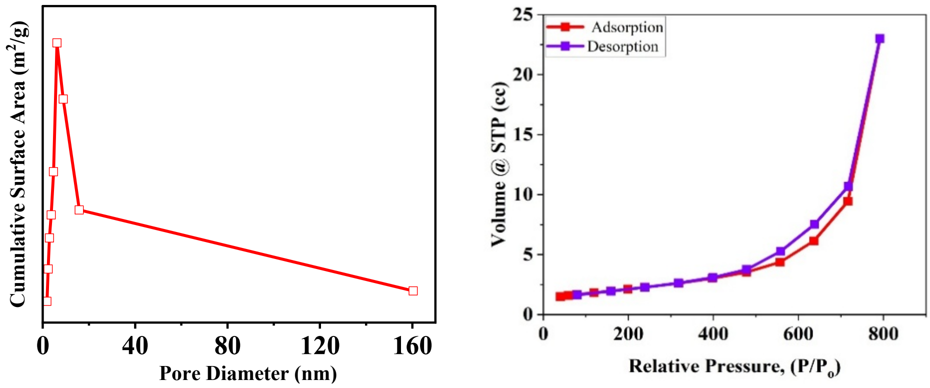

Figure 6. BET analysis of $NiFe_2O_4$ nanoparticles.

4.6. VSM Analysis

The room-temperature magnetization–field (M–H) hysteresis loop of the $NiFe_2O_4$ nanoparticles, as illustrated in Figure 7, demonstrates a sigmoidal shape indicative of ferrimagnetic ordering, recorded over a magnetic field range of ±2 T. The sample shows a saturation magnetization (M_s) of approximately 1.6 emu/g, with a low coercivity (Hc) of about 100–150 Oe and a small remanence (M_r) of approximately 0.12 memu, resulting in a squareness ratio (Mr/Ms) of roughly 3–4%. The observed reduction in M_s compared to that of bulk $NiFe_2O_4$, which typically ranges from 50 to 55 emu/g, can be attributed to the surface spin disorder that is characteristic of nanoscale ferrites. Furthermore, the low values of Hc and the M_r/M_s ratio suggest that the material exhibits soft ferrimagnetic properties, approaching near-superparamagnetic behavior, which is consistent with a particle size that is near the single-domain threshold.

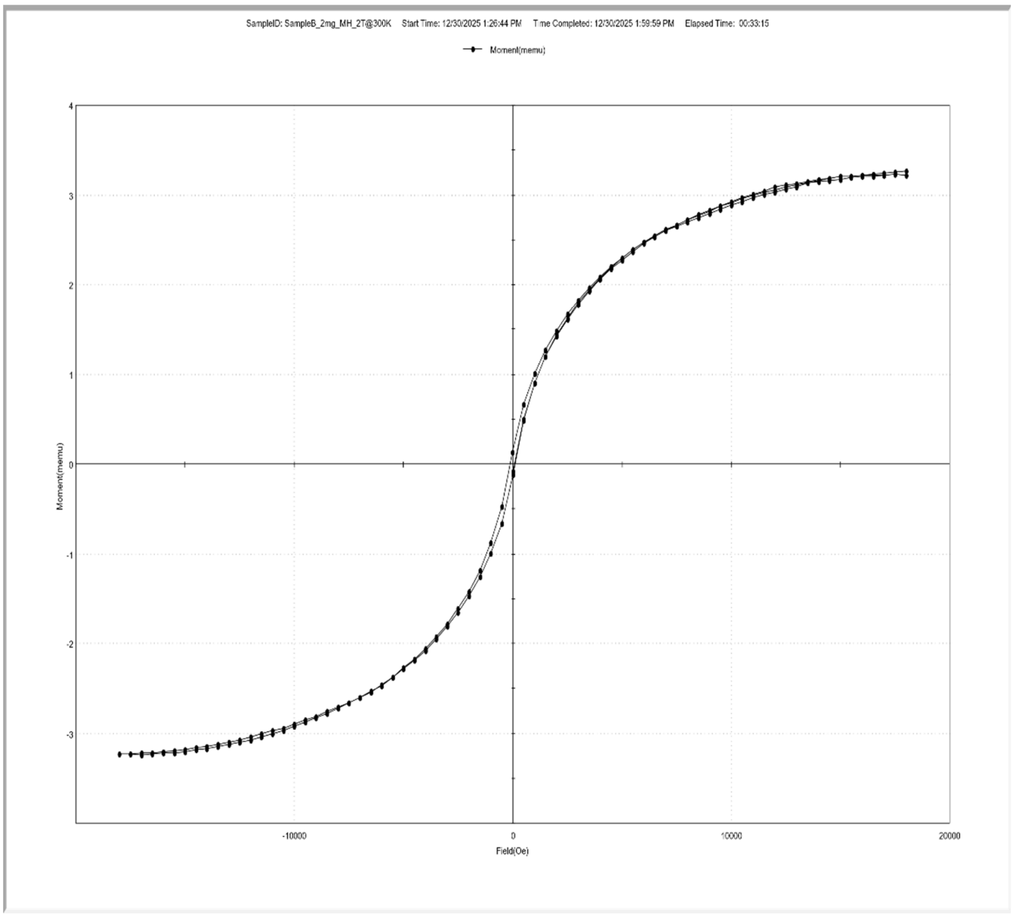

Figure 7. VSM analysis of $NiFe_2O_4$ nanoparticles.

5. Conclusions

In this study, we have developed a green and efficient protocol for the synthesis of $NiFe_2O_4$ nanocomposites using extract of Combretum indicum leaf, which is cost effective and easy to prepare. The synthesized catalyst was well-characterized by FT-IR, XRD, SEM, TEM, and BET. The catalytic system was highly active in the condensation of aromatic aldehydes with o-phenylenediamine in mild conditions at room temperature, providing high yields and short reaction times. This eco-friendly approach not only simplifies operations and allows for easy product separation but also uses a reusable and sustainable catalyst in line with green chemistry principles. The small, quasi-spherical particle size (12–18 nm) (Section 4.3), together with the moderate BET surface area of 49.82 m^2g^{-1} (Section 4.5), is consistent with a high density of accessible surface coordination sites, which is expected to favor substrate binding and facilitate the condensation/cyclization steps of the benzimidazole-forming reaction. A systematic study of how particle size and shape independently influence surface coordination and catalytic rate (e.g., by comparing catalyst batches annealed at different temperatures to vary crystallite size) was beyond the scope of the present work and is suggested as a direction for future studies.

Statement of the Use of Generative AI and AI-Assisted Technologies in the Writing Process

During the preparation of this manuscript, the authors used ChatGPT (OpenAI), QuillBot, and Claude in order to improve the language, grammar, and readability of the manuscript. After using these tools/services, the authors reviewed and edited the content as needed and take full responsibility for the content of the published article.

Acknowledgments

The authors are thankful to the Principal, MSS's Arts, Science and Commerce College, Ambad, Dist. Jalna, Maharashtra, India, for providing laboratory facilities.

Author Contributions

Conceptualization, K.T. and S.K.; Methodology, K.T.; Investigation, K.T. and S.K.; Writing—Original Draft Preparation, K.T.; Writing—Review & Editing, K.T. and S.K.; Supervision, S.K. All authors have read and agreed to the published version of the manuscript.

Ethics Statement

Not applicable.

Informed Consent Statement

Not Applicable.

Data Availability Statement

The data supporting the findings of this study are available within the article.

Funding

This research received no external funding.

Declaration of Competing Interest

The authors declare that they have no known competing financial interests or personal relationships that could have appeared to influence the work reported in this paper.

References

1. Kumar P, Tomar V, Kumar D, Joshi RK, Nemiwal M. Magnetically active iron oxide nanoparticles for catalysis of organic transformations: A review. *Tetrahedron* **2022**, *106–107*, 132641. DOI:10.1016/j.tet.2022.132641
2. Wang Y, Maksimuk S, Shen R, Yang H. Synthesis of iron oxide nanoparticles using a freshly-made or recycled imidazolium-based ionic liquid. *Green Chem.* **2007**, *9*, 1051. DOI:10.1039/b618933d
3. Horwat D, Zakharov DI, Endrino JL, Soldera F, Anders A, Migot S, et al. Chemistry, phase formation, and catalytic activity of thin palladium-containing oxide films synthesized by plasma-assisted physical vapor deposition. *Surf. Coat. Technol.* **2011**, *205*, S171–S177. DOI:10.1016/j.surfcoat.2010.12.021
4. Alsammarraie FK, Wang W, Zhou P, Mustapha A, Lin M. Green synthesis of silver nanoparticles using turmeric extracts and investigation of their antibacterial activities. *Colloids Surf. B Biointerfaces* **2018**, *171*, 398–405. DOI:10.1016/j.colsurfb.2018.07.059
5. Hoag GE, Collins JB, Holcomb JL, Hoag JR, Nadagouda MN, Varma RS. Degradation of bromothymol blue by 'greener' nano-scale zero-valent iron synthesized using tea polyphenols. *J. Mater. Chem.* **2009**, *19*, 8671. DOI:10.1039/b909148c
6. Baruwati B, Polshettiwar V, Varma RS. Glutathione promoted expeditious green synthesis of silver nanoparticles in water using microwaves. *Green Chem.* **2009**, *11*, 926. DOI:10.1039/b902184a
7. Saiqa Ikram SA. Silver Nanoparticles: One Pot Green Synthesis Using Terminalia arjuna Extract for Biological Application. *J. Nanomed. Nanotechnol.* **2015**, *6*, 1–6. DOI:10.4172/2157-7439.1000309
8. Devi HS, Boda MA, Shah MA, Parveen S, Wani AH. Green synthesis of iron oxide nanoparticles using *Platanus orientalis* leaf extract for antifungal activity. *Green Process. Synth.* **2019**, *8*, 38–45. DOI:10.1515/gps-2017-0145
9. Chahardoli A, Karimi N, Fattahi A. Nigella arvensis leaf extract mediated green synthesis of silver nanoparticles: Their characteristic properties and biological efficacy. *Adv. Powder Technol.* **2018**, *29*, 202–210. DOI:10.1016/j.apt.2017.11.003
10. Leili M, Fazlzadeh M, Bhatnagar A. Green synthesis of nano-zero-valent iron from Nettle and Thyme leaf extracts and their application for the removal of cephalexin antibiotic from aqueous solutions. *Environ. Technol.* **2018**, *39*, 1158–1172. DOI:10.1080/09593330.2017.1323956
11. Thovhogi N, Diallo A, Gurib-Fakim A, Maaza M. Nanoparticles green synthesis by Hibiscus Sabdariffa flower extract: Main physical properties. *J. Alloys Compd.* **2015**, *647*, 392–396. DOI:10.1016/j.jallcom.2015.06.076
12. Sone BT, Diallo A, Fuku XG, Gurib-Fakim A, Maaza M. Biosynthesized CuO nano-platelets: Physical properties & enhanced thermal conductivity nanofluidics. *Arab. J. Chem.* **2020**, *13*, 160–170. DOI:10.1016/j.arabjc.2017.03.004
13. Ehrampoush MH, Miria M, Salmani MH, Mahvi AH. Cadmium removal from aqueous solution by green synthesis iron oxide nanoparticles with tangerine peel extract. *J. Environ. Health Sci. Eng.* **2015**, *13*, 84. DOI:10.1186/s40201-015-0237-4
14. Kumar B, Smita K, Cumbal L, Debut A, Angulo Y. Biofabrication of copper oxide nanoparticles using Andean blackberry (*Rubus glaucus* Benth.) fruit and leaf. *J. Saudi Chem. Soc.* **2017**, *21*, S475–S480. DOI:10.1016/j.jscs.2015.01.009
15. Selvakesavan RK, Franklin G. Prospective Application of Nanoparticles Green Synthesized Using Medicinal Plant Extracts as Novel Nanomedicines. *Nanotechnol. Sci. Appl.* **2021**, *14*, 179–195. DOI:10.2147/NSA.S333467
16. Dhand V, Soumya L, Bharadwaj S, Chakra S, Bhatt D, Sreedhar B. Green synthesis of silver nanoparticles using Coffea arabica seed extract and its antibacterial activity. *Mater. Sci. Eng. C* **2016**, *58*, 36–43. DOI:10.1016/j.msec.2015.08.018
17. Gao JF, Li HY, Pan KL, Si CY. Green synthesis of nanoscale zero-valent iron using a grape seed extract as a stabilizing agent and the application for quick decolorization of azo and anthraquinone dyes. *RSC Adv.* **2016**, *6*, 22526–22537. DOI:10.1039/C5RA26668H
18. Jeevanandam J, Chan YS, Danquah MK. Biosynthesis of Metal and Metal Oxide Nanoparticles. *ChemBioEng Rev.* **2016**, *3*, 55–67. DOI:10.1002/cben.201500018
19. Eker F, Akdaşçi E, Duman H, Bechelany M, Karav S. Green Synthesis of Silver Nanoparticles Using Plant Extracts: A Comprehensive Review of Physicochemical Properties and Multifunctional Applications. *Int. J. Mol. Sci.* **2025**, *26*, 6222. DOI:10.3390/ijms26136222
20. Castillo-Henríquez L, Alfaro-Aguilar K, Ugalde-Álvarez J, Vega-Fernández L, Montes de Oca-Vásquez G, Vega-Baudrit JR. Green Synthesis of Gold and Silver Nanoparticles from Plant Extracts and Their Possible Applications as Antimicrobial Agents in the Agricultural Area. *Nanomaterials* **2020**, *10*, 1763. DOI:10.3390/nano1009176
21. Kamyab H, Khalili E, Khademi T, Yuzir A, Taheri MM, Rajendran S, et al. Advances in green synthesis of nanoparticles for biomedical applications: Antimicrobial, antiviral, and cancer therapies. *Mater. Today Sustain.* **2026**, *33*, 101287. DOI:10.1016/j.mtsust.2025.101287
22. Bhardwaj B, Singh P, Kumar A, Kumar S, Budhwar V. Eco-Friendly Greener Synthesis of Nanoparticles. *Adv. Pharm. Bull.* **2020**, *10*, 566–576. DOI:10.34172/apb.2020.067

23. Devesa S. *Comparative Overview of Metal Oxide Nanoparticle Synthesis Methods: Conventional Sol-Gel Versus Green Approaches*; Intechopen: London, UK, 2025. DOI:10.5772/intechopen.1008457
24. Hashem HE, El Bakri Y. An overview on novel synthetic approaches and medicinal applications of benzimidazole compounds. *Arab. J. Chem.* **2021**, *14*, 103418. DOI:10.1016/j.arabjc.2021.103418
25. Rajabi F, De S, Luque R. An Efficient and Green Synthesis of Benzimidazole Derivatives Using SBA-15 Supported Cobalt Nanocatalysts. *Catal. Lett.* **2015**, *145*, 1566–1570. DOI:10.1007/s10562-015-1546-z
26. Tahlan S, Ramasamy K, Lim SM, Shah SAA, Mani V, Narasimhan B. 4-(2-(1H-Benzo[d]imidazol-2-ylthio)acetamido)-N-(substituted phenyl)benzamides: Design, synthesis and biological evaluation. *BMC Chem.* **2019**, *13*, 12. DOI:10.1186/s13065-019-0533-7
27. Tahlan S, Ramasamy K, Lim SM, Shah SAA, Mani V, Narasimhan B. Design, synthesis and therapeutic potential of 3-(2-(1H-benzo[d]imidazol-2-ylthio)acetamido)-N-(substituted phenyl)benzamide analogues. *Chem. Cent. J.* **2018**, *12*, 139. DOI:10.1186/s13065-018-0513-3
28. Achar KCS, Hosamani KM, Seetharamareddy HR. *In-vivo* analgesic and anti-inflammatory activities of newly synthesized benzimidazole derivatives. *Eur. J. Med. Chem.* **2010**, *45*, 2048–2054. DOI:10.1016/j.ejmech.2010.01.029
29. Gaba M, Gaba P, Uppal D, Dhingra N, Bahia MS, Silakari O, et al. Benzimidazole derivatives: Search for GI-friendly anti-inflammatory analgesic agents. *Acta Pharm. Sin. B* **2015**, *5*, 337–342. DOI:10.1016/j.apsb.2015.05.003
30. Camacho J, Barazarte A, Gamboa N, Rodrigues J, Rojas R, Vaisberg A, et al. Synthesis and biological evaluation of benzimidazole-5-carbohydrazide derivatives as antimalarial, cytotoxic and antitubercular agents. *Bioorganic Med. Chem.* **2011**, *19*, 2023–2029. DOI:10.1016/j.bmc.2011.01.050
31. Desai NC, Shihory NR, Kotadiya GM, Desai P. Synthesis, antibacterial and antitubercular activities of benzimidazole bearing substituted 2-pyridone motifs. *Eur. J. Med. Chem.* **2014**, *82*, 480–489. DOI:10.1016/j.ejmech.2014.06.004
32. Starčević K, Kralj M, Ester K, Sabol I, Grce M, Pavelić K, et al. Synthesis, antiviral and antitumor activity of 2-substituted-5-amidino-benzimidazoles. *Bioorganic Med. Chem.* **2007**, *15*, 4419–4426. DOI:10.1016/j.bmc.2007.04.032
33. Wang XJ, Xi MY, Fu JH, Zhang FR, Cheng GF, Yin DL, et al. Synthesis, biological evaluation and SAR studies of benzimidazole derivatives as H1-antihistamine agents. *Chin. Chem. Lett.* **2012**, *23*, 707–710. DOI:10.1016/j.cclet.2012.04.020
34. Monforte AM, Ferro S, De Luca L, Lo Surdo G, Morreale F, Pannecouque C, et al. Design and synthesis of N1-aryl-benzimidazoles 2-substituted as novel HIV-1 non-nucleoside reverse transcriptase inhibitors. *Bioorganic Med. Chem.* **2014**, *22*, 1459–1467. DOI:10.1016/j.bmc.2013.12.045
35. Alpan AS, Parlar S, Carlino L, Tarikogullari AH, Alptüzün V, Güneş HS. Synthesis, biological activity and molecular modeling studies on 1H-benzimidazole derivatives as acetylcholinesterase inhibitors. *Bioorganic Med. Chem.* **2013**, *21*, 4928–4937. DOI:10.1016/j.bmc.2013.06.065
36. Andrzejewska M, Yepez-Mulia L, Tapia A, Cedillo-Rivera R, Laudy AE, Starościak BJ, et al. Synthesis, and antiprotozoal and antibacterial activities of S-substituted 4,6-dibromo- and 4,6-dichloro-2-mercaptobenzimidazoles. *Eur. J. Pharm. Sci.* **2004**, *21*, 323–329. DOI:10.1016/j.ejps.2003.10.024
37. Wang M, Han X, Zhou Z. New substituted benzimidazole derivatives: A patent review (2013–2014). *Expert Opin. Ther. Pat.* **2015**, *25*, 595–612. DOI:10.1517/13543776.2015.1015987
38. Yao C, Lei S, Wang C, Li T, Yu C, Wang X, et al. Three-component synthesis of 4-aryl-1*H*-pyrimido[1,2-*a*]benzimidazole derivatives in ionic liquid. *J. Heterocycl. Chem* **2010**, *47*, 26–32. DOI:10.1002/jhet.215
39. Sapkal S, Shelke K, Sonar S, Shingate B, Shingare M. Acidic ionic liquid catalyzed environmentally friendly synthesis of benzimidazole derivatives. *Bull. Catal. Soc. India* **2009**, *2*, 78–83. Available online: https://www.researchgate.net/profile/Suryakant Sapkal/publication/237474967_Acidic_ionic_liquid_catalyzed_environmentally_friendly_synthesis_of_benzimidazole_derivatives/links/02e7e533d32d784ce1000000/Acidic-ionic-liquid-catalyzed-environmentally-friendly-synthesis-of-benzimidazole-derivatives.pdf (accessed on 1 January 2009).
40. Matinise N, Kaviyarasu K, Mongwaketsi N, Khamlich S, Kotsedi L, Mayedwa N, et al. Green synthesis of novel zinc iron oxide ($ZnFe_2O_4$) nanocomposite via Moringa Oleifera natural extract for electrochemical applications. *Appl. Surf. Sci.* **2018**, *446*, 66–73. DOI:10.1016/j.apsusc.2018.02.187
41. Mayedwa N, Mongwaketsi N, Khamlich S, Kaviyarasu K, Matinise N, Maaza M. Green synthesis of zin tin oxide ($ZnSnO_3$) nanoparticles using Aspalathus Linearis natural extracts: Structural, morphological, optical and electrochemistry study. *Appl. Surf. Sci.* **2018**, *446*, 250–257. DOI:10.1016/j.apsusc.2017.12.161
42. Bashir AKH, Matinise N, Sackey J, Kaviyarasu K, Madiba IG, Kodseti L, et al. Investigation of electrochemical performance, optical and magnetic properties of $NiFe_2O_4$ nanoparticles prepared by a green chemistry method. *Phys. E Low-Dimens. Syst. Nanostruct.* **2020**, *119*, 114002. DOI:10.1016/j.physe.2020.114002

43. Matinise N, Botha N, Madiba IG, Maaza M. Mixed-phase bismuth ferrite oxide ($BiFeO_3$) nanocomposites by green approach as an efficient electrode material for supercapacitor application. *MRS Adv.* **2023**, *8*, 703–707. DOI:10.1557/s43580-023-00603-4
44. Matinise N, Mayedwa N, Kaviyarasu K, Nuru ZY, Madiba IG, Mongwaketsi N, et al. Zinc zirconate ($ZnZrO_3$) nanocomposites bimetallic designed by green synthesis via Moringa Olefeira extract for high-performance electrochemical applications. *Mater. Today Proc.* **2021**, *36*, 401–407. DOI:10.1016/j.matpr.2020.04.743
45. Sontakke VA, Ghosh S, Lawande PP, Chopade BA, Shinde VS. A Simple, Efficient Synthesis of 2-Aryl Benzimidazoles Using Silica Supported Periodic Acid Catalyst and Evaluation of Anticancer Activity. *ISRN Org. Chem.* **2013**, *2013*, 453682. DOI:10.1155/2013/453682
46. Kumar SK, Rao AL, Rani AP, Mounika GN, Ramya JS. Aluminium chloride catalyzed one-pot synthesis of 2-aryl substituted benzimidazoles and their antibacterial activity. *Asian J. Pharm. Anal.* **2023**, *4*, 198–202. Available online: https://www.researchgate.net/profile/Srikanth-Kumar-Karumanchi-2/publication/375186750_Aluminium_chloride_catalyzed_one-pot_synthesis_of_2-aryl_substituted_benzimidazoles_and_their_antibacterial_activity/links/6543528d0426ef6369f56b56/Aluminium-chloride-catalyzed-one-pot-synthesis-of-2-aryl-substituted-benzimidazoles-and-their-antibacterial-activity.pdf (6 January 2014).
47. Kusuma S, Bawiskar DB, Singh C, Panneerselvam P, Sinha P, Samal AK, et al. Facile one pot synthesis of 2-substituted benzimidazole derivatives under mild conditions by using engineered MgO@DFNS as heterogeneous catalyst. *RSC Adv.* **2023**, *13*, 32110–32125. DOI:10.1039/D3RA05761E
48. Ananya Shenoy AM. *Combretum Indicum* Linn. A Comprehensive Review of Phytochemistry and Pharmacological Properties. *Int. J. Pharm. Sci.* **2025**, *3*, 1825–1831. DOI: 10.5281/zenodo.15050292
49. Matinise N, Fuku XG, Kaviyarasu K, Mayedwa N, Maaza M. ZnO nanoparticles via Moringa oleifera green synthesis: Physical properties & mechanism of formation. *Appl. Surf. Sci.* **2017**, *406*, 339–347. DOI:10.1016/j.apsusc.2017.01.219
50. Mayedwa N, Mongwaketsi N, Khamlich S, Kaviyarasu K, Matinise N, Maaza M. Green synthesis of nickel oxide, palladium and palladium oxide synthesized via Aspalathus linearis natural extracts: physical properties & mechanism of formation. *Appl. Surf. Sci.* **2018**, *446*, 266–272. DOI:10.1016/j.apsusc.2017.12.116
51. Nwanya AC, Ndipingwi MM, Mayedwa N, Razanamahandry LC, Ikpo CO, Waryo T, et al. Maize (*Zea mays* L.) fresh husk mediated biosynthesis of copper oxides: Potentials for pseudo capacitive energy storage. *Electrochim. Acta* **2019**, *301*, 436–448. DOI:10.1016/j.electacta.2019.01.186
52. Karunakaran G, Jagathambal M, Van Minh N, Kolesnikov E, Kuznetsov D. Green Synthesis of $NiFe_2O_4$ Spinel-Structured Nanoparticles Using Hydrangea paniculata Flower Extract with Excellent Magnetic Property. *JOM* **2018**, *70*, 1337–1343. DOI:10.1007/s11837-018-2871-7